Biochimica et Biophysica Acta 1850 (2015) 1107–1119

Contents lists available at ScienceDirect

Biochimica et Biophysica Acta

journal homepage: www.elsevier.com/locate/bbagen

Amyloidogenic lysozymes accumulate in the endoplasmic reticulum accompanied by the augmentation of ER stress signals

Yoshiki Kamada [a], Takahiro Kusakabe [b], Yasushi Sugimoto [a,*]

[a] Laboratory of Biochemistry and Bioscience, The United Graduate School of Agricultural Sciences, Kagoshima University, Kagoshima 890-0065, Japan
[b] Laboratory of Sericultural Science, Graduate School of Agricultural Sciences, Kyushu University, Fukuoka 812-8581, Japan

ARTICLE INFO

Article history:
Received 24 July 2014
Received in revised form 21 January 2015
Accepted 27 January 2015
Available online 4 February 2015

Keywords:
Lysozyme
Mutants
Amyloidosis
Endoplasmic reticulum
ER stress

ABSTRACT

Background: Naturally occurring single mutants, I56T, F57I, W64R and D67H of lysozyme in human, have been known to form abnormal protein aggregates (amyloid fibrils) and to accumulate in several organs, including the liver, spleen and kidney, resulting in familial systemic amyloidosis. These human pathogenic lysozyme variants are considered to raise subtle conformational changes compared to the wild type.
Methods: Here we examined the effects of the aberrant mutant lysozymes I56T, F57I, W64R and D67H, each of which possesses a point mutation in its molecule, on a cultured human cell line, HEK293, in which the genes were individually integrated and overexpressed.
Results: Western blot analyses showed lesser amounts of these variant proteins in the medium compared to the wild type, but they were abundant in the cell pellets, indicating that the modified lysozyme proteins were scarcely secreted into the medium but were retained in the cells. Immunocytochemistry revealed that these proteins resided in restricted regions which were stained by an endoplasmic reticulum (ER) marker. Moreover, the overexpression of the mutant lysozymes were accompanied by marked increases in XBP-1s and GRP78/BiP, which are downstream agents of the IRE1α signaling pathway responding to the unfolded protein response (UPR) upon ER stress. RNAi for the mutant lysozymes' expression greatly suppressed the increases of these agents.
Conclusions and General significance: Our results suggest that the accumulation of pathogenic lysozymes in the ER caused ER stress and the UPR response mainly via the IRE1α pathway.

1. Introduction

Accumulations of abnormal proteins that are misfolded and fibrotic have been observed in cases of pathological amyloidosis such as Alzheimer's disease, Parkinson's disease, prion diseases, type II diabetes and lysozyme-related diseases [1–5]. None of the proteins involved in these diseases have common amino acid sequences or tertiary structures, but each of them can form amyloid fibrils consisting of a cross β-sheet structure and can be deposited in various tissues [6,7]. These proteins form an oligomer or intermediate after becoming unfolded, aggregated and finally limbless amyloid-like fibrils [8,9], which are toxic in most but not all cases. This complicated situation has stimulated research into the causal link between amyloid fibrils and disease [10,11]. Amyloid beta peptide (Aβ), associated with the cause of Alzheimer's disease, was shown to be cytotoxic, and it was reported that its early aggregations (oligomers) as well as its prefibrillar aggregates have stronger cytotoxicity than the mature fibrils themselves [12]. Such fibril polymorphisms can result from the protein aggregation of misfolded monomers and oligomers with distinct conformational characteristics.

Lysozyme is an omnipresent enzyme attacking the peptidoglycan cell wall of certain microorganisms by the selective hydrolysis of the β-1,4 glycosidic linkages between the N-acetylmuramic acid and N-acetylglucosamine [13,14]. There are at most five pathologic mutants of human lysozyme that cause non-neuropathic systemic amyloidosis. Naturally occurring single mutants, I56T, F57I, W64R and D67H (Fig. 1), have been known to form abnormal protein aggregates (amyloid fibrils) and to accumulate in several organs, including the liver, spleen

Abbreviations: Armet, arginine-rich, mutated in early stage tumors; ATF4, activating transcription factor 4, a PERK downstream target; ATF6α, activating transcription factor 6α; CHOP, C/EBP homologous protein; DAPI, diamidino-2-phenylindole; EDEM1, ER degradation-enhancing α-mannosidase-like protein1; eIF2α, eukaryotic initiation factor 2α; ER, endoplasmic reticulum; ERdj4, a member of ER-resident DnaJ family chaperones; GADD45, growth arrest and DNA damage-inducible protein; GAPDH, glyceraldehyde-3-phosphate dehydrogenase; GRP78/BiP, glucose regulated protein 78/binding immunoglobulin protein; GRP94, a member of ER-resident Hsp90 family chaperones; HEDJ, an Hsp40 co-chaperone localized to the ER; HRD1, HMG-CoA reductase degradation 1 homolog; IRE1, inositol-requiring enzyme 1; $p58^{IPK}$, potential negative regulator of eIF2α signaling; p-eIF2α, phosphorylated eIF2α; PDI, protein disulfide isomerase; PERK, double stranded RNA activated protein kinase (PKR)-like endoplasmic reticulum kinase; RNAi, RNA interference; UPR, unfolded protein response; *XBP-1*, X-box binding protein 1 mRNA; XBP-1s, protein from the spliced XBP-1 mRNA; *XBP-1u*, unspliced XBP-1 transcript

* Corresponding author. Tel./fax: +81 99 285 8781.
E-mail address: yasushi@chem.agri.kagoshima-u.ac.jp (Y. Sugimoto).

http://dx.doi.org/10.1016/j.bbagen.2015.01.018
0304-4165/

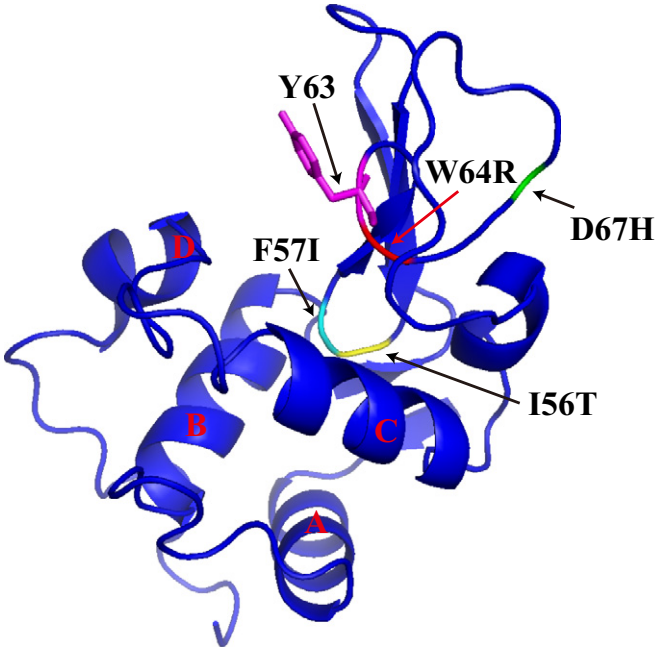

Fig. 1. Structure of human wild-type lysozyme. The locations of the four amyloidogenic single-point mutations, I56T, F57I, W64R and D67H, as well as Y63 which is crucial for the fibril formation, are marked by arrows and colored residues. A–D: helices. The structure was reproduced by using PDB (1LZ1) and PyMOL [27].

and kidney, resulting in amyloidosis [15]. These human pathogenic lysozyme variants are considered to raise subtle conformational changes compared to the wild type.

In addition, it has been reported that lysozyme mutants are apt to make amyloid fibrils in vitro [16]. Human lysozyme is a secretory protein that, like most other secretory proteins, is present in body fluid and extracellular tissues. Whether the secretory conditions of mutant lysozyme proteins, that may not have normal functions, are changed or not is of interest. The relationships of secretion with a number of destabilized human lysozyme variants have been studied thoroughly in *Pichia pastoris*[16]; these proteins showed extensively decreased levels of secretion. The issue as to the stability and secretion status of human lysozyme mutants was also pursued in a *Drosophila melanogaster* system created by the authors [17].

In the present study, we overexpressed the above-described four pathogenic lysozyme mutants (I56T, F57I, W64R and D67H) in cultured human embryonic kidney (HEK) 293 cells. These proteins were present mainly in the insoluble fraction of the cell homogenate. We observed an accumulation of the expressed lysozyme mutants in the restricted intracellular area assigned to the endoplasmic reticulum (ER), and examined whether the accumulation of aberrant proteins were accompanied by the increases of ER stress signals.

2. Materials and methods

2.1. Cell line and reagents

The HEK293 cell line was from RIKEN BRC (Tsukuba, Japan). Human lysozyme and other chemical reagents were obtained from Wako Fine Chemicals (Osaka, Japan). The antibodies used were purchased as follows: Anti-lysozyme and anti-protein disulfide isomerase (PDI) antibodies from Abcam (Cambridge, MA); anti-glyceraldehyde-3-phosphate dehydrogenase (GAPDH) and anti-vimentin antibodies from Santa Cruz Biotechnology (Santa Cruz, CA); anti-γ-tubulin and anti-Golgi 58K from Sigma-Aldrich (St. Louis, MO); anti-XBP-1s antibody from Biolegend (San Diego, CA); anti-p-eIF2α and anti-cleaved caspase-3 antibodies from Cell Signaling Technology (Beverly, MA); and anti-ATF6 antibody from BioAcademica (Osaka, Japan). Anti-GRP78/BiP antibody was from R&D Systems (Minneapolis, MN) for western blotting and Santa Cruz Biotechnology for immunocytochemistry, respectively. The secondary antibodies used for each first antibody were HRP-binding antibody (Jackson Immuno Research, WestGrove, PA) and Alexa Fluor 488a- or 546-conjugated IgG (H + L) (Life Technologies, Carlsbad, CA).

2.2. Expression vectors

Lysozyme cDNA containing signal sequence was obtained from a human leukocyte cDNA library and inserted into pENTRY™11 vector. Four lysozyme mutant cDNAs were made by using a KOD-plus mutagenesis kit (Toyobo, Osaka, Japan) from the above cDNA. The obtained sequences were inserted into the pEBMulti-neo expression vector (Wako) with *EcoRV* and *Kpn1* restriction sites and used for transfection.

2.3. Transfection, gene expression and analyses

HEK293 cells were cultured in Dulbecco's Modified Eagle's Medium (DMEM; Wako) with fetal bovine serum (FBS; Thermo Scientific HyClone, Logan, UT), NEAA (Gibco, Grand Island, NY) and Antibiotic–antimycotic (Gibco) in a 5% CO_2 humidified atmosphere at 37 °C. The sub-confluent cells (1.5×10^6 cells/35-mm) were then incubated in the same medium overnight. After the medium was replaced with Opti MEM (Gibco) medium and incubated for 1 h, the cells were transfected with plasmid DNA using the X-tremeGENE HP (Roche Diagnostics, Indianapolis, IN) and incubated for 72 h. The positive controls for ER stress and caspase-3 were made by treating the cells with tunicamycin or camptothecin (both Sigma) at a concentration of 2 or 7 μg/ml, respectively.

The cells were subjected to the isolation of total RNAs with TRIzol® reagent (Life Technologies), which were subjected to reverse transcription-polymerase chain reaction (RT-PCR) using adequate primers. After electrophoresis, the PCR products were observed with the ChemiDoc XRS system (Bio-Rad Laboratories, Hercules, CA). For the cell viability test, the transiently transfected cells were placed in a 24-well plate at an intensity of 5×10^5 cells/well, incubated at 37 °C for 72 h with occasional changes of medium, and analyzed using the Guava ViaCount viability assay kit (Millipore, Bedford, MA) according to the manufacturer's instructions. Quantitative real-time PCR was performed by the PCR Cycler (TAKARA-Bio, Otsu, Japan). Analyses were made for mRNAs of lysozyme, GRP78/BiP etc., as well as the total, uncut and spliced *XBP-1* sequences with appropriate designed primers (Suppl. Table. S1) designed according to the Primer blast (Integrated DNA Technologies, Coralville, Iowa). Data were normalized to GAPDH. For the RNAi and immunocytochemical studies, the incubation conditions of the cells were modified as described below.

2.4. RNA interference

HEK293 cells (1.5×10^6/well) were seeded in six-well plates, preincubated for 24 h and cotransfected with the mixture of the vector-bearing lysozyme sequence and that bearing a 21-nucleotide double-strand RNA in the presence of X-tremeGENE siRNA as a transfection reagent. The double-strand RNA applied was 5′-*UUUUGACAACGA UUUCUCCAU*-3′/5′-*GGAGAAAUCG UUGUCAAAACA*-3′, which corresponds to the 387–409 sequences of lysozyme. The culture medium used was DMEM with FBS and non-essential amino acids (NEAAs). After a 72-h incubation, the cells were collected and used for the western blot analysis and RT-PCR.

2.5. Western blot analysis

Cells were homogenized with a lysis buffer containing 10 mM Tris–HCl buffer, pH 7.4, 1% NP-40 and protease inhibitor cocktail

(Roche Diagnostics). After centrifugation at 14,000 *g* for 20 min, the supernatant (lysate) and pellet were subjected to western blotting with the antibody (see above). The medium was also analyzed. Prior to the analysis, specimens were adjusted to provide equal concentrations of protein using the Micro BCA protein assay system (Thermo/Pierce, Rockford, IL). Immunoblots were visualized using ECL reagent, and the rough protein quantity in the immunoreactive bands was estimated using Image Lab™ Software (Bio-Rad) against a house-keeping protein, GAPDH. The relative values of the ER stress were obtained by the protein quantities in the bands as described above.

2.6. Immunofluorescence and microscopy

The transiently transfected cells were cultured on a collagen-coated coverglass (25-mm dia.) for 72 h and washed three times with phosphate-buffered saline (PBS), followed by fixation in 4% paraformaldehyde in PBS or 10% trichloroacetic acid (TCA) at 25 °C for 15 min. After permeabilization with 0.2% Triton X-100 in PBS for 10 min, the cells were incubated with a blocking solution consisting of 10% goat serum or 1% bovine serum albumin in TBS-T (0.1% Tween 20) for 30 min, followed by incubation at 4 °C overnight with the adequate first antibody.

If necessary, the cells were washed three times with PBS and incubated for 1 h with the secondary antibody diluted in blocking solution. After three washes in PBS, the coverglass was mounted on a glass slide in Prolong Gold antifade reagent (Life Technologies) and viewed on a confocal laser microscope (Nikon EZC-1) using an excitation wavelength of 488 nm or 546 nm. The images were merged using Adobe Photoshop (Adobe Systems). For the detection of aggregates, we used the ProteoStat® Aggresome Detection Kit (Enzo Life Sciences, New York, NY) according to the protocol provided by the maker. Some of the transfected cells were treated with MG-132 for 12 h before incubation. The cells were counterstained with DAPI.

3. Results

3.1. Cell viability

First, the wild-type lysozyme and the four mutant lysozymes I56T, F57I, W64R and D67H (Fig. 1) were overexpressed for 72 h in HEK293 cells, which were then collected and subjected to flow cytometry (Table 1). The expression of both wild-type and mutant lysozyme genes brought about a division into approx. 8–9 to 1 viable versus apoptotic plus nonviable cell populations. These results were roughly similar to those obtained in mock experiments. The proportion of nonviable cells for the W64R mutant lysozyme was the highest among the samples listed in the table, although the result was not reproducible in another series of experiments (data not shown).

3.2. Presence of overexpressed lysozymes in and out of the cells

Next, we tested the gene expression and distribution of products in the HEK293 cells with the wild-type and four mutant lysozyme genes. Lysozyme mRNAs were detected in all of the specimens except the mock (Fig. 2, top panel). As seen in the western blot data for the culture medium (Fig. 2, third panel), the wild-type lysozyme conferred a strong signal, indicating that the protein was extensively secreted (≥0.5 μg/ml medium), whereas the four mutants did not, with a trace band in each medium.

In contrast, the pellet fraction from the wild type exhibited a weak band, but the same fractions from the mutants displayed strong bands (Fig. 2, fifth panel). Cell lysates from both the wild-type and mutant specimens gave signals which were slightly stronger in the latter than the former (Fig. 2, fourth panel). These results indicated the occurrence of a more marked intracellular retention of mutant lysozyme proteins compared to the wild type.

Table 1
Viable, apoptotic and non-viable HEK293 cells were identified by differential fluorescence by Guava Viacount® and flow cytometry.

	Viable cells (%)	Apoptotic cells (%)	Non-viable cells (%)
Mock	87.9 ± 0.9	3.4 ± 0.2	8.7 ± 1.0
Wild	86.9 ± 0.8	5.1 ± 0.2	8.0 ± 0.7
I56T	87.0 ± 0.5	5.1 ± 0.3	8.0 ± 0.5
F57I	87.7 ± 1.1	5.0 ± 0.6	7.4 ± 0.6
W64R	84.8 ± 0.4	5.2 ± 0.3	10.0 ± 0.3
D67H	86.3 ± 1.2	5.2 ± 0.1	8.5 ± 1.2

Statistic analysis of the Viacount® assay (n = 4). Date expressed as mean ± SE.

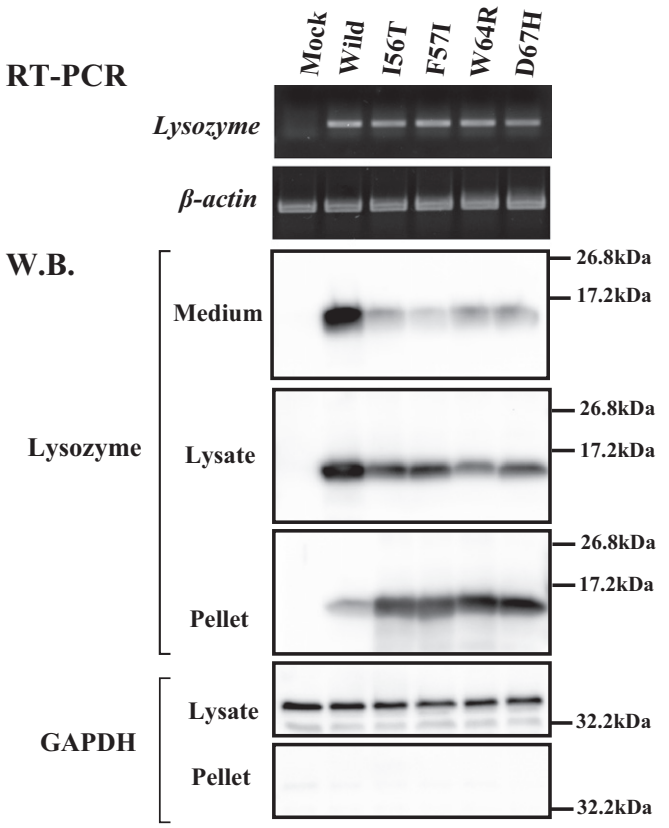

Fig. 2. Expression of wild-type and mutant lysozyme genes introduced into HEK293 cells, which were incubated for 72 h after transfection. Mock, cells transfected with vector alone; Wild, the cells transfected with wild-type lysozyme gene; I56T etc., the cells transfected with the four mutants (Fig. 1). *Top two panels*: RT-PCR results for lysozymes as well as for internal β-actin as a control. *Bottom five panels*: Western blots of the cultured media, cell lysates and cell pellets (from top to the third panels, respectively) using the anti-human lysozyme antibody. The migration rate coincided with that of an authentic lysozyme (not shown). The bottom two panels represent the analysis of internal GAPDH as a control. No lysozyme expression was detected in the Mock. The nuclear fractions of all of the specimens contained scarcely any lysozymes (not illustrated). Right numbers denote protein size markers. All results shown here were reproducible in three cycles of experiments.

3.3. Localization of aberrant lysozyme in the cell

Although lysozymes are considered secretory proteins, the lysozyme signal was found in the insoluble fraction of cells, especially in the mutants (cf. Fig. 2). To investigate the intracellular distribution of lysozyme, we optically observed the HEK293 cells expressing the wild-type and mutant lysozymes by staining with the human lysozyme antibody (Fig. 3). The wild-type lysozyme presented rather equivocal cytoplasmic distribution, whereas the mutant lysozymes in all of the specimens tested were found in definite intracellular areas, which were thought to represent protein accumulation. This inference was supported by the

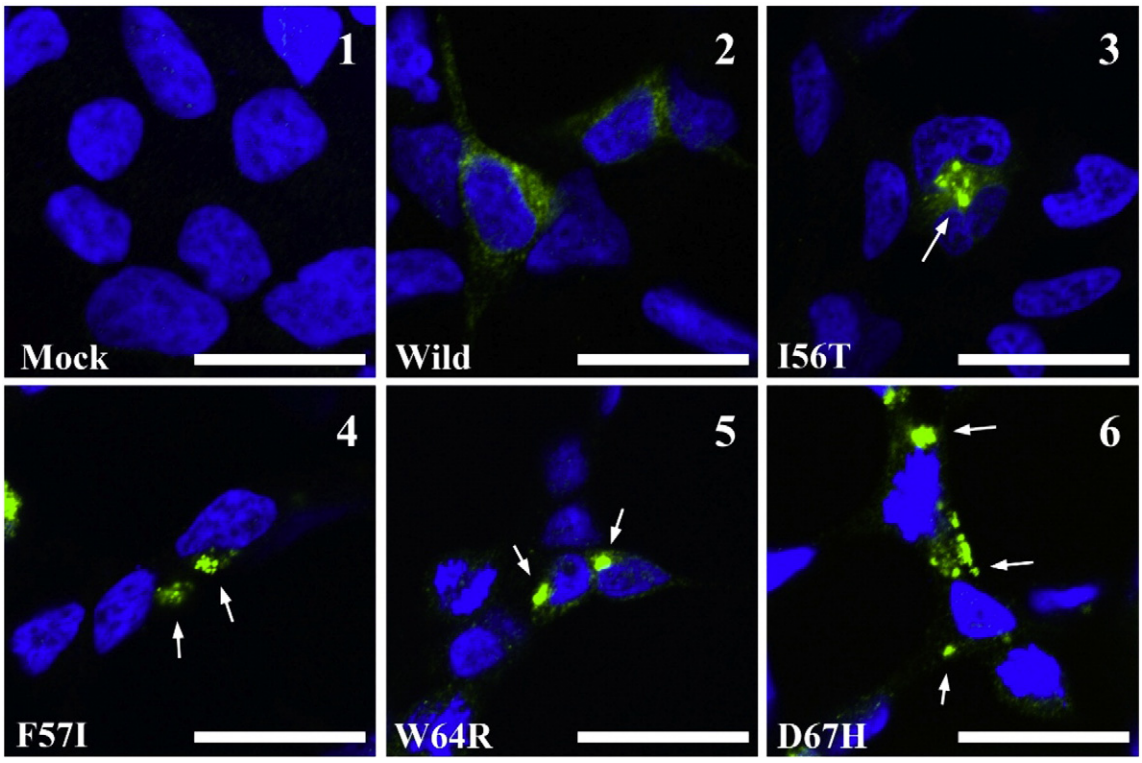

Fig. 3. Localization of lysozyme proteins expressed in HEK293 cells. Transfected cells (incubated for 72 h) were fixed, labeled with Alexa 488-conjugated secondary IgG against anti-lysozyme antibody (green) and observed by confocal laser microscopy. For Mock, Wild and I56T etc., see Fig. 2 legend. Arrows point to the regions of mutant lysozyme accumulation. Scale bar: 20 μm. These results were reproducible in three cycles of experiments.

results of the protein-aggregation-detection test with ProteoStat (Fig. 4, middle panels), wherein the positive regions were in accord with the localization of the lysozyme signal (Fig. 4, top and bottom panels). On the other hand, the cells with the wild-type lysozyme did not give strong signals for this test (Fig. 4, 'Wild' panels). These findings support the idea that the lysozyme variant proteins overexpressed in the cells were secreted only slightly into the culture medium and the majority accumulated in limited regions of the cytoplasm, probably forming some type of aggregates.

However, these accumulations, although being ProteoStat-positive, could not be attributed to the so-called aggresomes formed as inclusion bodies in the cytosol, since the lysozyme regions were not coincident with the signals for the two aggresome components γ-tubulin and vimentin as probes (Fig. 5A,B). We then examined the mutant lysozymes

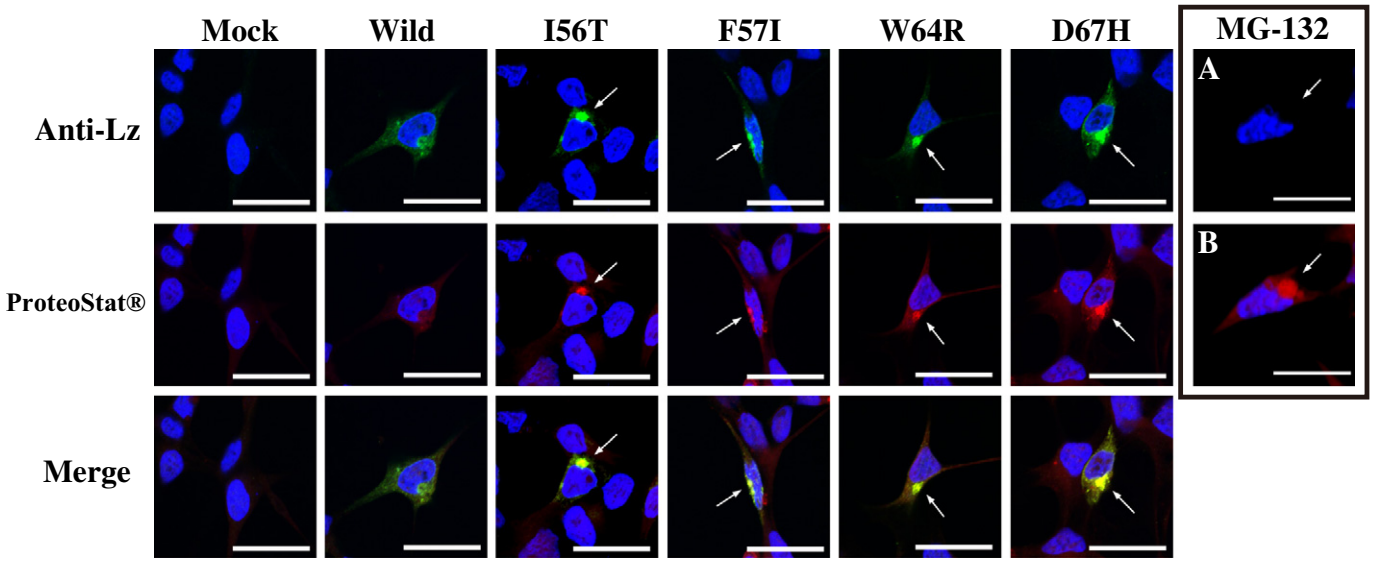

Fig. 4. Localization of lysozyme proteins in the ProteoStat-positive regions. Transfected HEK293 cells (incubated for 72 h) were fixed and double-labeled with Alexa 488-conjugated secondary IgG against anti-lysozyme antibody (green) and an aggresome detection kit (red), followed by observation by confocal laser microscopy. *Top panels*: Detection of lysozyme. *Middle*: Detection of putative aggresomes. *Bottom*: Superimposed images. MG-132; proteosome inhibitor as a positive control. See Fig. 2 legend for other details. Similar results were given by three cycles of experiments. A, DAPI; B, DAPI plus ProteoStat. Scale bar: 20 μm.

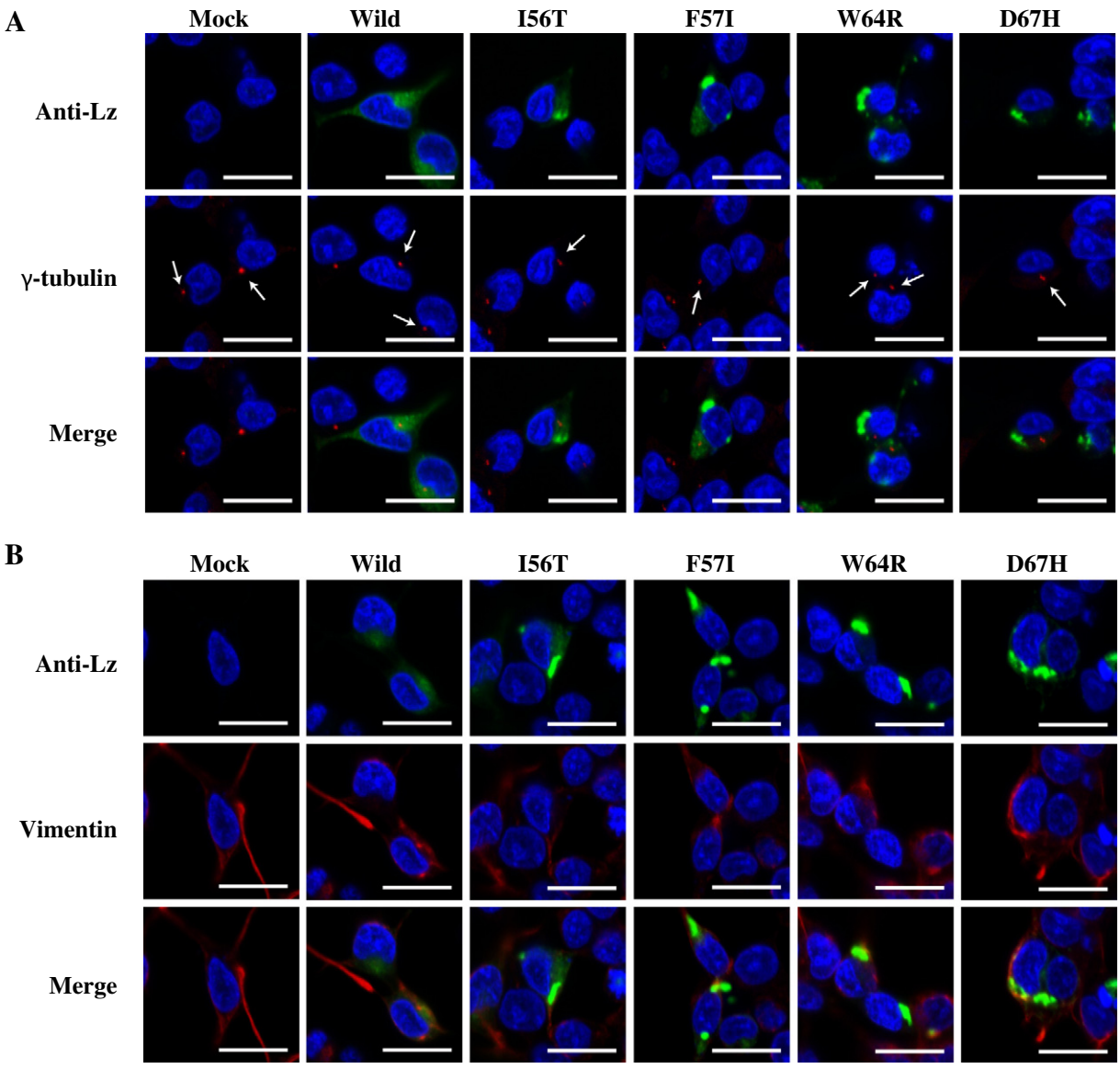

Fig. 5. Localization of lysozyme proteins in the areas not positive for γ-tubulin and vimentin signals. Transfected HEK293 cells (incubated for 72 h) were fixed and double-labeled with Alexa 488-conjugated secondary IgG against anti-lysozyme antibody (green) and an antibody against either of the two aggresome components γ-tubulin or vimentin (red), and observed by confocal laser microscopy. *Top* panels of A and B, detection of lysozyme. *Middle* panels of A, detection of γ-tubulin. White arrows show positions of γ-tubulin. *Middle* panels of B, detection of vimentin. *Bottom* panels of A and B, superimposed images. See Fig. 3 legend for other details. These results were reproducible in three cycles of experiments. Scale bar: 20 μm.

to elucidate whether these exist in the ER or Golgi body, using PDI and Golgi 58K as markers, respectively. The regions of lysozymes were in good agreement with the ER signal (Fig. 6A) but did not overlap with that of the Golgi (Fig. 6B). These data suggested the possibility that the aberrant lysozymes accumulate mainly in the ER. Therefore, our subsequent subject of investigation was the possible involvement of the unfolded protein response (UPR) and ER stress, both of which are generally related to the deposition of denatured or disordered proteins.

3.4. Search for indications of the UPR and ER stress

We first attempted to detect GRP78/BiP, which is known to be a responding sensor to the UPR. Western blots (Fig. 7A) indicated that GRP78/BiP was abundant in the cell lysates in which its apparent levels were hardly different among all of the specimens tested. Interestingly, the bands of GRP78/BiP in the cell pellets of the mutants were at an intensity comparable to that in the lysates, while the bands for the wild-type and mock specimens were much weakened. Moreover, the immunocytochemical staining (Fig. 7B) showed that the signal regions for GRP78/BiP merged fully with those for the four lysozyme mutants. We infer that the UPR activation was occurring where the mutant lysozymes accumulated in the cells.

Secondly, we investigated whether any other symptom of ER stress was augmented by the deposition of aberrant lysozymes. It has been accepted that, when unfolded proteins are sequestered by GRP78/BiP, ER-transmembrane transducers including IRE1, PERK and ATF6 are activated. As seen in Fig. 8, the IRE1's downstream effector XBP-1s, i.e., the translation product of spliced X-box binding protein 1 mRNA, exhibited a definite difference between the wild-type and mutant lysozymes, with stronger band intensity in the latter than in the former (second panel). However, both the downstream members of PERK and ATF6, i.e., unphosphorylated/phosphorylated eukaryotic initiation factor 2 (eIF2α and p-eIF2α, respectively) and full-length/cleaved activating transcription factor (ATF6α), were hardly altered between the wild type and mutants (Fig. 8, third to fifth panels). Likewise, the cleaved caspase-3 was unchanged in band intensity (Fig. 8, sixth panel). Rough quantitation of these ER stress signaling (see the numerals in Fig. 8) supported the above observations. Results of pharmacological

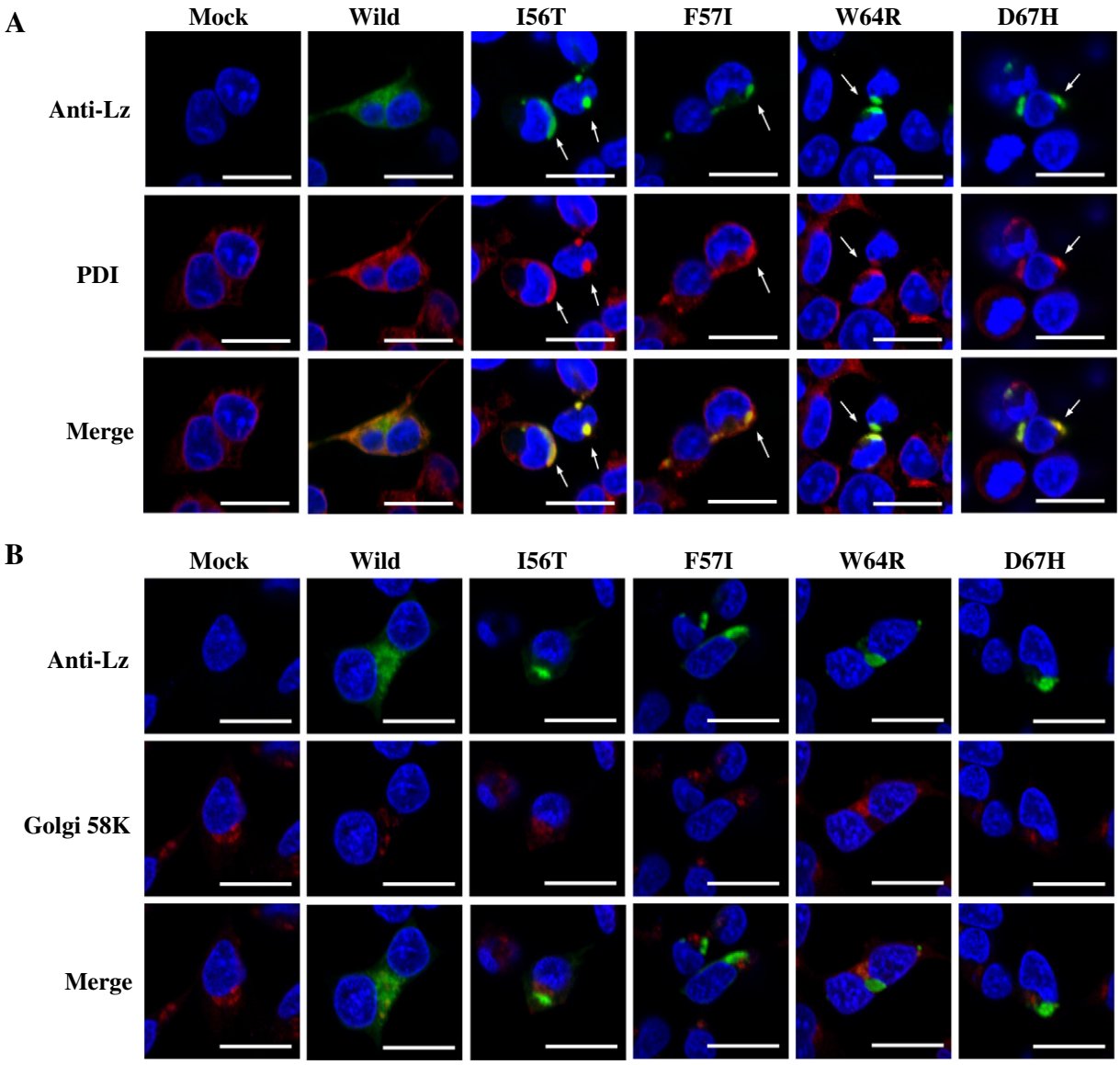

Fig. 6. Localization of lysozyme proteins in the areas positive for PDI signal but not for Golgi 58K signal. Transfected HEK293 (incubated for 72 h) cells were fixed and double-labeled with Alexa 488-conjugated secondary IgG against anti-lysozyme antibody (green) and either of the antibodies for PDI (an ER marker) and Golgi 58K (a Golgi body component) (red), followed by confocal laser microscopy. *Top* panels of A and B, detection of lysozyme. *Middle* panels of A, detection of PDI. *Middle* panels of B, detection of Golgi 58K. *Bottom* panels of A and B, superimposed images. See Fig. 3 legend for other details. Reproducible results were obtained in three cycles of experiments. Scale bar: 20 μm.

induction of ER stress by using tunicamycin were positive, indicating that the response sensors as far as tested were potentially active in the HEK cells (cf. the rightmost two lanes in second to sixth panels of Fig. 8).

We then quantified, by real-time PCR, the transcripts of the ER stress-related UPR genes in the current specimens, and results are illustrated in Fig. 9A and B. The levels of *XBP-1s* and *GRP78/BiP* elevated significantly, as much as 2-fold, in the mutant cells compared to the mock and wild-type cells. Also augmented were the data of *ERdj4*, *HEDJ* and *GRP94*, whose products might somehow be related to the IRE1–XBP-1–BiP pathway. In addition, expressions of several genes such as $p58^{IPK}$ (down-regulator of eIF2a–ATF4 pathway) and *Armet* (inhibitor of stress-induced cell death) showed a tendency to be augmented, sometimes over 1.5-fold. *ATF4*, an indicator of the PERK pathway, hardly moved, while $p58^{IPK}$, which is a depressor of PERK, rose to some extent (Fig. 9B). Although *CHOP* was increased, its translation product CHOP (downstream factor of the PERK pathway) did not exhibit changes (data not shown). Thus, the overall signals for the degradation of unfolded proteins and apoptosis seemed to be inert in the cells expressing the lysozyme variants. This was in agreement with the observations shown in Table 1 and Fig. 8. Taken together with the above-described results, the data suggest that the overexpression of mutant lysozymes brought about ER stress accompanied by the activation of the IRE1–XBP-1–BiP pathway.

3.5. RNAi for lysozyme mRNAs

To further test the inference that ER stress and the resulting activation of XBP-1 occurred, we examined the effects of lysozyme RNAi on the expression of relevant transcripts and proteins by RT-PCR and western blot, respectively. We confirmed that, by RNAi, the mutant lysozyme transcripts declined (Fig. 10, top panel of A) and that the lysozyme proteins decreased in the cell pellets (Fig. 10, third panel of B). In the mutant specimens, the bands of spliced *XBP-1* (*XBP-1s*) were also clearly downregulated by RNAi, whereas the band of the unspliced one (*XBP-1u*) increased (Fig. 10, second panel of A). In addition, GRP78/BiP, which increased in the cells harboring mutant lysozymes,

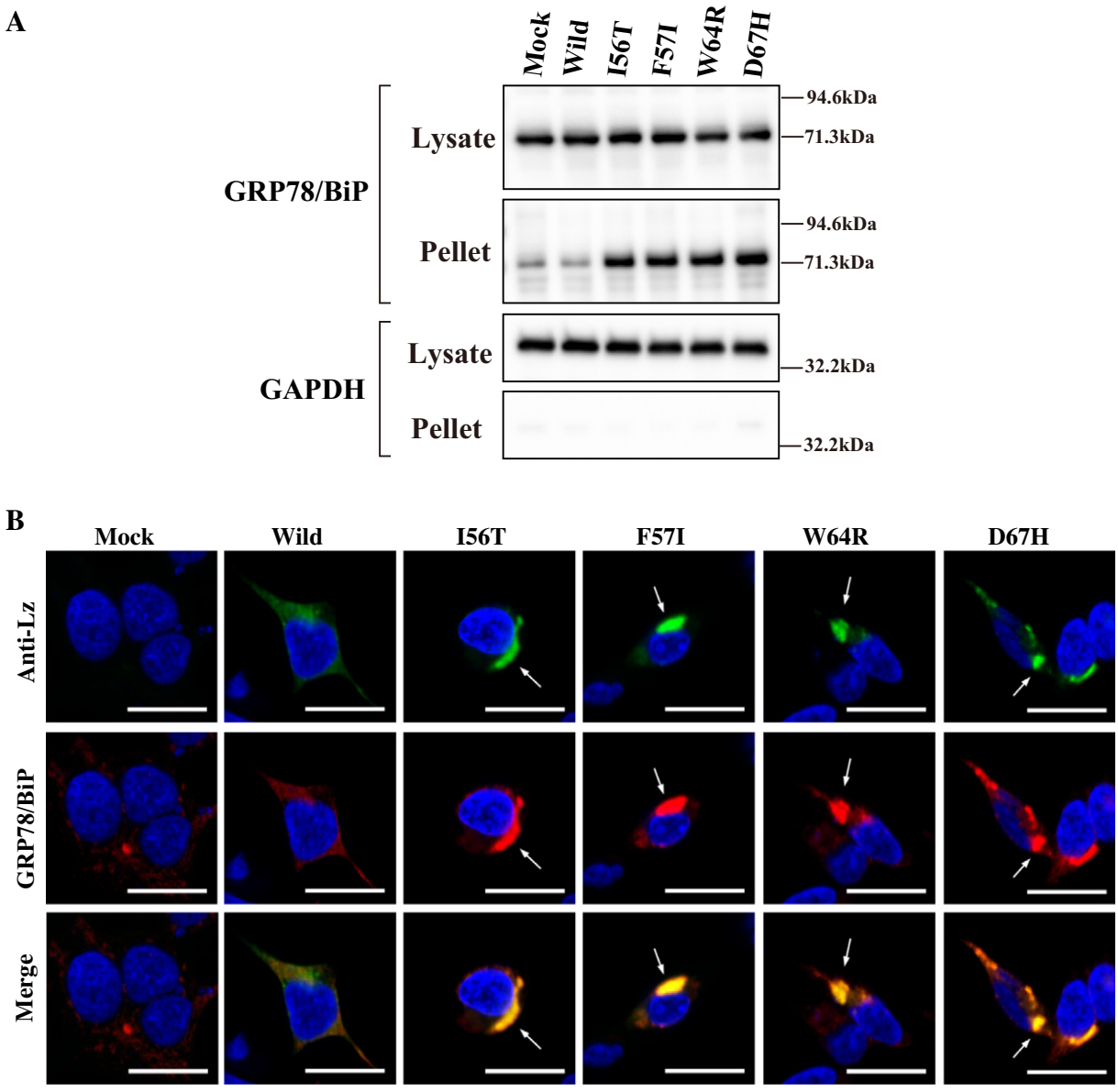

Fig. 7. Detection and localization of GRP78/BiP in HEK293 cells transfected with lysozyme genes (incubated for 72 h). A: Western blot with the human GRP78/BiP-specific antibody. *Top* panel: cell lysates. *Second* panel: cell pellets. *Bottom* two panels: The expression of an internal control (see Fig. 2). Right numbers denote protein size markers. B: Localization of lysozyme proteins in the GRP78/BiP-positive regions. The cells were fixed and double-labeled with Alexa 488-conjugated secondary IgG against anti-lysozyme antibody (green) and the anti-GRP78/BiP antibody (red), followed by confocal laser microscopy. *Top* panels: Detection of lysozyme. *Middle* panels: Detection of GRP78/BiP. *Bottom* panels: Superimposed images. See Fig. 3 legend for other details. Overall results were reproducible in three cycles of experiments. Scale bar: 20 μm.

was observed to have declined considerably in the pellets of mutant cells by RNAi (Fig. 10, fifth panel of B). The overall results indicated that the overexpression of aberrant lysozymes induced ER stress and its response, which were reduced by the decreased gene expression by RNAi.

4. Discussion

The folding process or its failure of wild-type and mutant lysozymes has been studied in detail [15,18–21]. Regarding the variants of human lysozyme used in the present examination (I56T, F57I, W64R and D67H; Fig. 1), the mutation sites are concentrated in the position surrounding the core region at the β-domain [16], of which nine amino acids (55G–63Y) are indispensable for amyloid fibril formation [22,23]. Comparisons of the conformational structures of these lysozymes (our unpublished results and refs. [24,25]) indicated that, in each of the mutants, the core region is more extruded toward the surface than is the case in the wild type. In the native state, these lysozyme variants are thought to have a destabilized structure and a propensity for misfolding, aggregation and fibril formation.

To further clarify the deleterious effects of such lysozymes on cells, we constructed expression vectors bearing these human lysozyme mutants and introduced each into HEK293 cells. The genes were expressed well but had no significant effects on viability of cells in comparison to the wild type. Also apoptosis was hardly observed under the present experimental conditions as shown above, although the cells were observed to begin apoptosis in the case of incubation over 72 h after transfection (the experiments here were carried out at the incubation time of 72 h since the gene expression tested was maximum at this period). These results were somewhat different from the previous results that exogenously added agents, such as amyloid protein oligomers or proto-fibrils and mature fibrils, brought about cytotoxicity and accompanied apoptosis to cultured cells [12,26]. The problems pertinent to fibril formation and apoptosis are discussed further below.

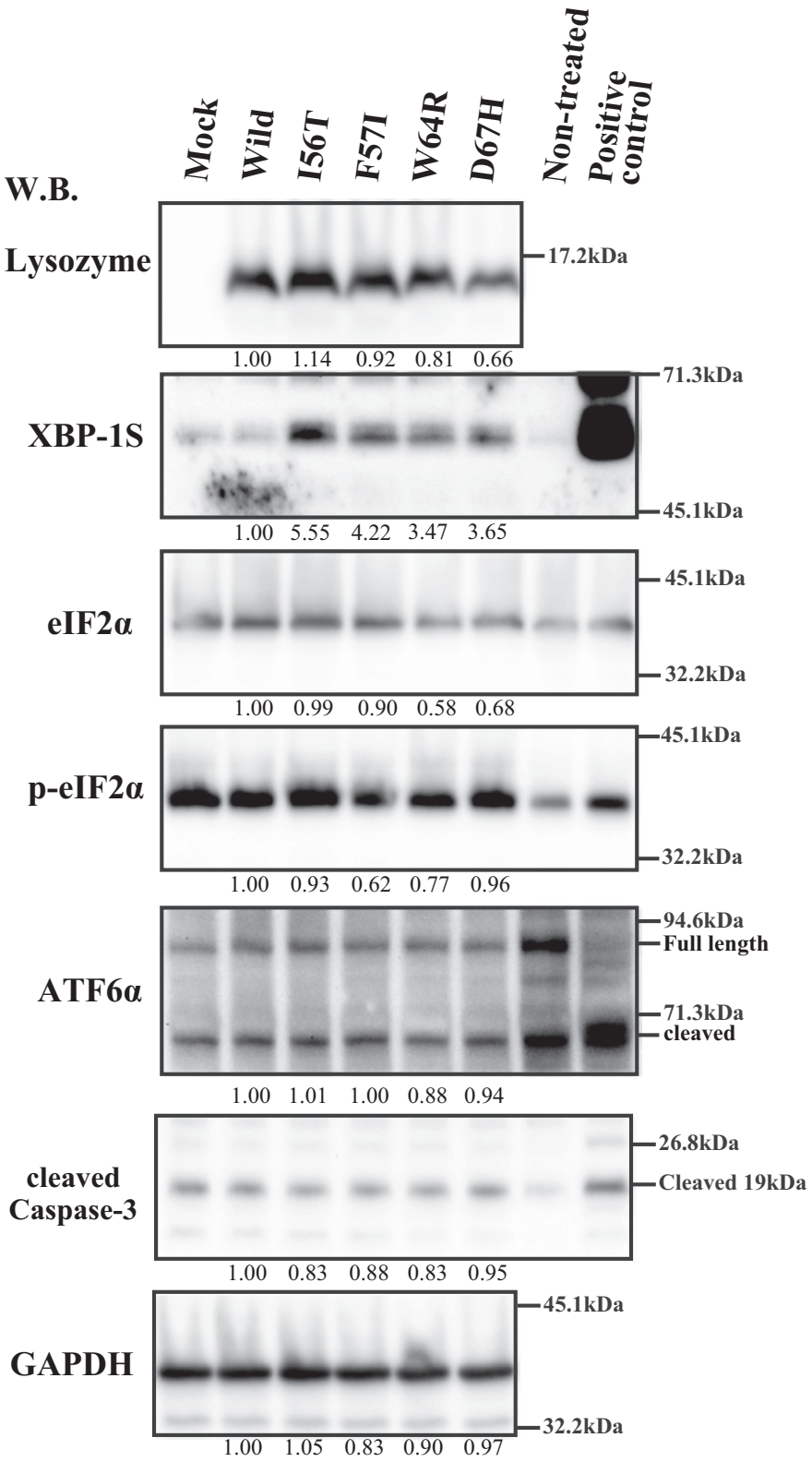

Fig. 8. Detection of ER stress factors in HEK293 cells transfected with lysozyme genes (incubated for 72 h). A western blot analysis was carried out for total cell lysates. *Top* panel: Detection of lysozyme. *Second*: Detection of XBP-1s. *Third*: Detection of eIF2α. *Fourth*: Detection of p-eIF2α. *Fifth*: Detection of full-length and cleaved 3ATP6α. *Sixth*: Detection of cleaved caspase-3. See Fig. 2 legend for other details. Right numbers denote protein size markers. Reproducible results were obtained in three cycles of experiments. The *positive control* lanes in the second to sixth panels depict the patterns after treatment of intact cells (having no transfection vector) with an inducer camptothecin (7 μg/ml for cells) for the activation of caspase or with another inducer tunicamycin (2 μg/ml for cells) for the activation of other effectors. The *non-treated* lanes represent specimens treated similarly but without the inducer. Numbers under each panel represent the intensity ratios toward that of the wild-type specimen.

In mouse L cells, misfolding mutants of human lysozyme had previously reported to be retained, eventually degraded by cysteine protease in a pre-Golgi compartment and associated with protein disulfide isomerase [27]. A recent report using *P. pastoris* shows that the less stable variants of human lysozyme are kept within the cell and targeted for degradation, therefore leading to less amount of secretion [28]. Similarly, the four types of amyloidogenic lysozymes overexpressed in the HEK293 cells were less secreted into the medium compared to the wild type, remaining in the insoluble fraction, but they were accumulated within definite regions of cells as described above. Our results suggest that the degradation of aberrant lysozymes is much slower in HEK293 cell than in the mouse L cells or *P. pastoris*. Additionally, another lysozyme mutant, T70N, was found to be well secreted outside the cells, giving a weak band in the cell pellets, just like the wild type (Supplemental Fig. S1). This may be related to the fact that T70N is a non-amyloidogenic mutant, thought to be present in the British population with an allele frequency of 5% [29]. It is not known whether T70N can undergo normal folding processes, and studies on the subject are underway in our laboratory.

Occasionally, cells accumulate a lot of misfolded proteins without degradation. In this manner, cells may escape from toxic effects due to protein aggregates. It has been indicated that misfolded polyubiquitinated protein aggregates are recruited and transported to a cytoplasmic structure termed aggresomes, which are surrounded by vimentin via the microtubule network containing γ-tubulin [30–32]. In the present study, however, despite being positive for the aggresome detection kit, the intracellular regions where the present aberrant lysozymes exist did not match the signal regions for vimentin or γ-tubulin. In addition, the mutant lysozymes in the pellet fractions of cells may not be ubiquitinated, since these exhibited a single band with the migration rate similar to that of intact lysozyme (Fig. 2, fifth panel). Thus, we concluded that the present four lysozyme mutants did not form aggresomes in terms of the strict definition.

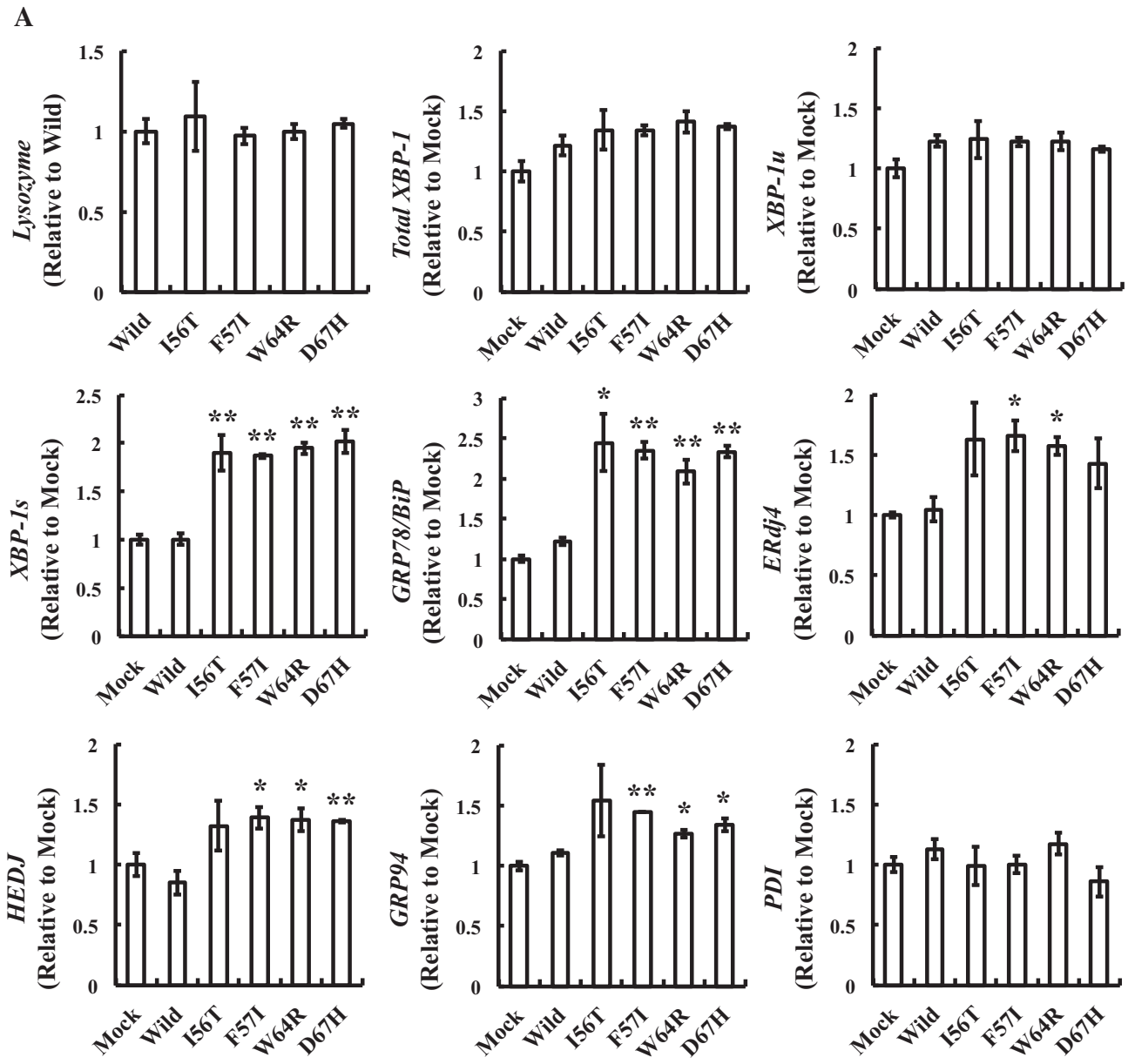

Fig. 9. Expression of ER-stress transcripts by the introduction of lysozyme variants as measured by quantitative real-time PCR. HEK293 cells incubated at 37 °C for 72 h were used. Patterns for *lysozyme*, *XBP-1* (total), *XBP-1u*, *XBP-1s*, *GRP78/BiP*, *ERdj4*, *HEDJ*, *GRP94*, *PDI* are shown in panel *A*, and those for *ATF4*, *p58*^{IPK}, *HRD1*, *GADD45*, *calnexin*, *EDEM1*, *CHOP* and *Armet* are in panel B. Data were normalized against the housekeeping GAPDH and are represented by means ± SEM of 3 independent experiments. The values of lysozyme variants differing significantly versus those of the wild-type specimen are marked by * or ** ($P < 0.05$ and $P < 0.01$, respectively).

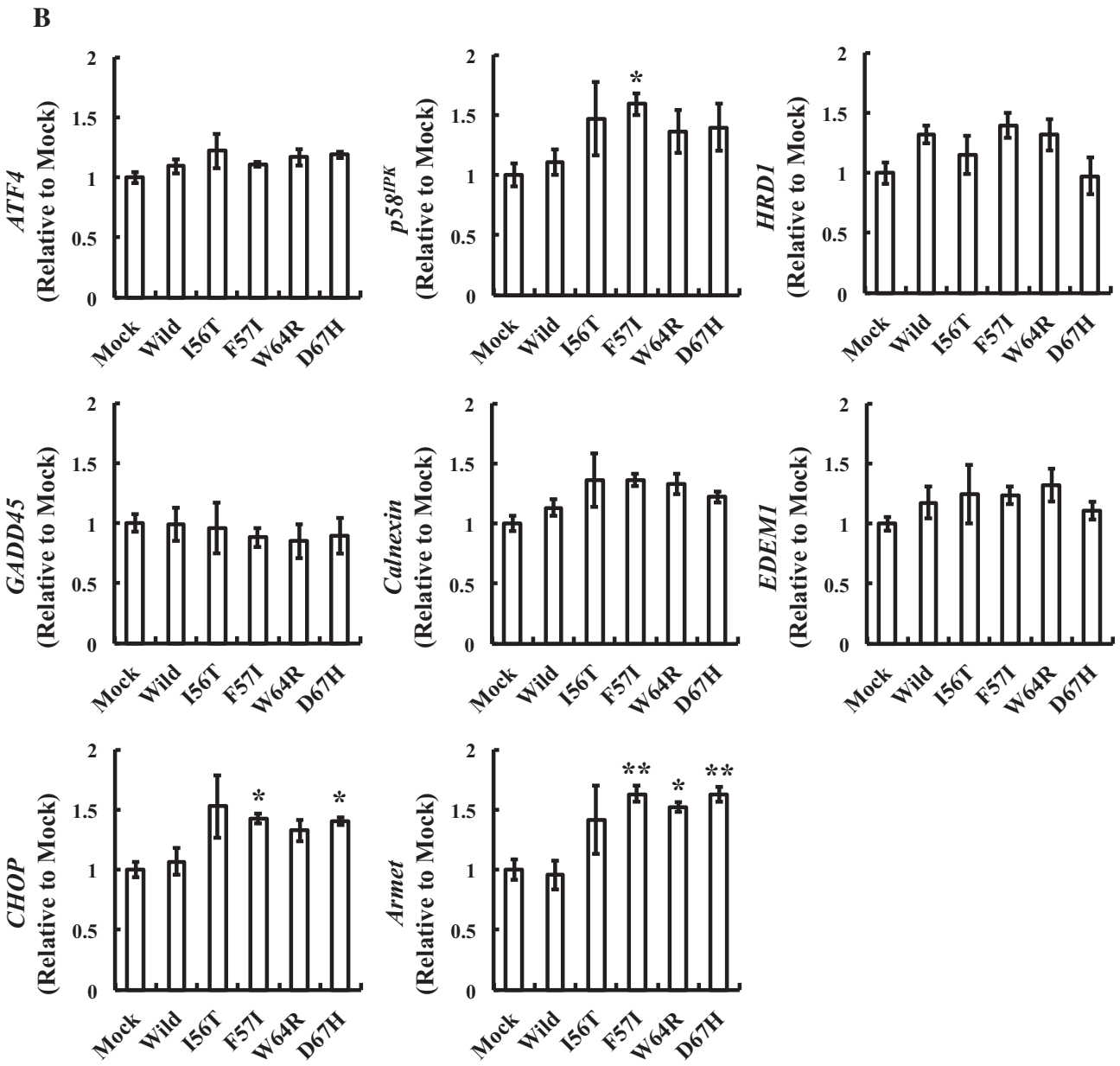

Fig. 9 (*continued*).

In general, aberrant proteins such as those that fail to undergo folding are accumulated in the ER under conditions in which the ER stress response is taking place. Sometimes ER stress is evoked by the deposition of misfolding protein in the ER as seen in the present case. ER stress stimulates the UPR, which is the adaptive process that reduces the stress by retrieving the protein folding homeostasis [33–36]. The UPR is conveyed by ER transmembrane sensors such as IRE1α, PERK and ATF6 [34,37–40]. Molecular chaperons are necessary for correct folding to overexpression of a large amount of abnormal lysozyme. GRP78/BiP, one of the major players of the UPR, is known to bind IRE1 in the ER when there is no stress. According to the general concept [36,41–43], appearance of abnormal protein leads to the dissociation of GRP78/BiP-IRE1, thereby IRE1 forms a dimer in the ER membrane, exhibits the RNase activity and splices the uncut *XBP-1*, which produces active *XBP-1s*. Its translation product XBP-1s has been reported to lure molecular chaperones under the control of the ER stress response element (ERSE) [44]. We suppose that such processes took place in the present cells. In parallel with the increase of GRP78/BiP, related molecular chaperone transcripts examined elevated clearly by the lysozyme variants as described above. Some of the relevant factors are known to function against the cell death or the PERK pathway. It is inferred that the so-called ER-associated protein degradation (ERAD) system for aberrant protein and the stress-mediated apoptosis system was promoted solely to a limited extent under the present conditions of our cells. So far, only the response of the signal pathway involving XBP-1 and GRP78/BiP was clearly shown. More studies are needed to determine the participation of other signaling network agents (including IRE1β).

Moreover, *XBP-1s*, the spliced form of mature mRNA *XBP-1u*, was distinctly increased by the overexpression of lysozyme variants (Fig. 10A, second panel). These results were verified by RNAi for mutant lysozymes expression, whose reduction was in concert with the lack of IRE1 activation and of the GRP78/BiP amount together with a marked decrease of insoluble lysozymes. GRP78/BiP, as a molecular chaperone, is said to correct the structure of denatured proteins, although we could not confirm that this effect took place in the cells that we used.

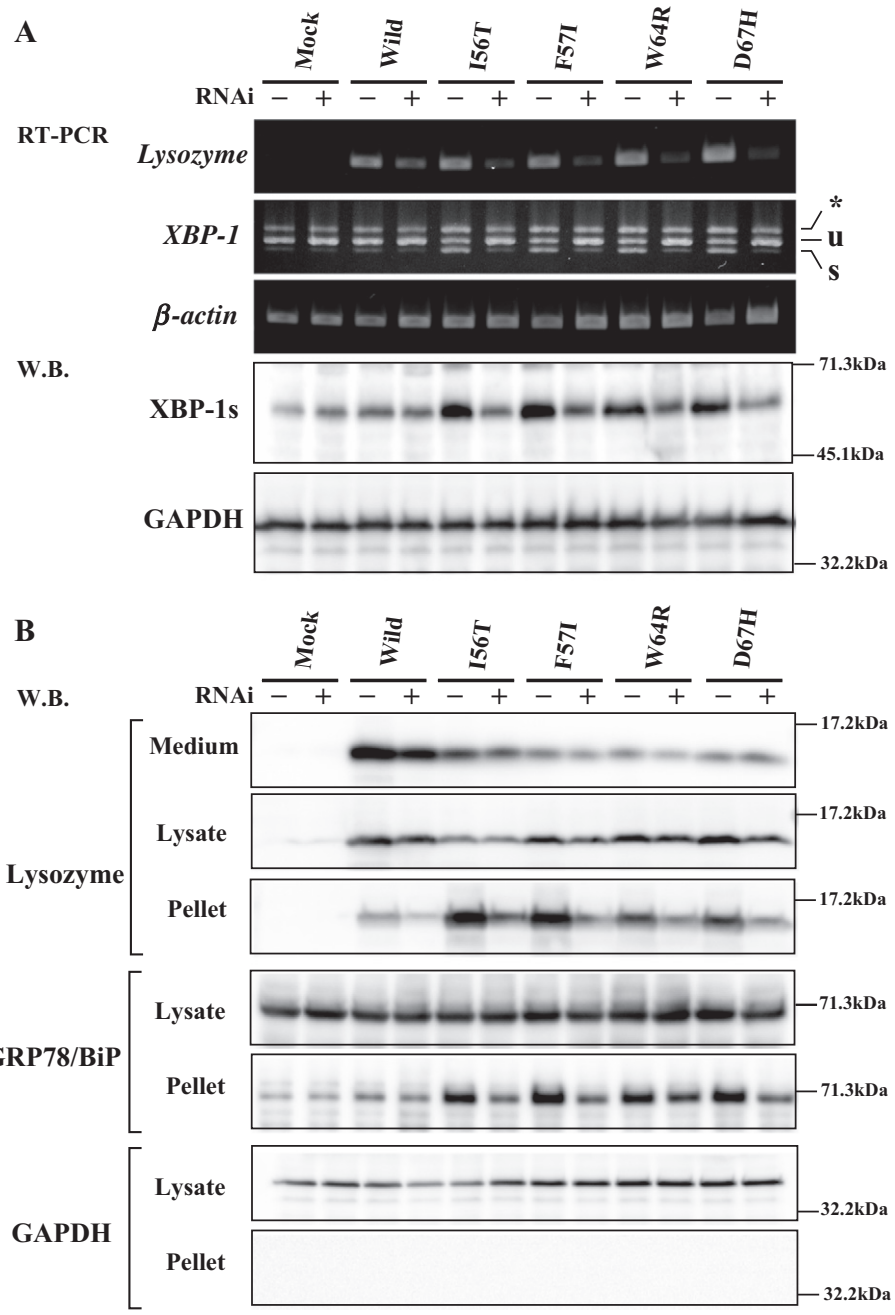

Fig. 10. Suppression of ER stress by RNAi for lysozyme gene expression in transfected HEK293 cells (incubated for 72 h). (−), without RNAi; (+) with RNAi. A: Analyses of splicing for XBP-1 mRNA and its product in cell lysates. *Top* panel: RT-PCR for lysozyme mRNA. *Second*: RT-PCR for *XBP-1*, where u, s and * denote unspliced, spliced and total (combined data), respectively [39]. *Fourth*: The western blot for XBP-1s (spliced *XBP-1* product). B: Western blot for lysozyme in media, cell lysates and pellets (*top*, *second* and *third* panels, respectively) and for GRP78/BiP in cell lysates and pellets (*fourth* and *fifth* panels, respectively). β-Actin and GAPDH (mRNA and/or protein) were analyzed as internal controls in A and B. For other details see Fig. 2 legend. The overall results were reproducible in three cycles of experiments.

It is of interest to know whether GRP78/BiP interacts with aberrant lysozymes in the ER. Does GRP78/BiP remain bound to lysozymes? This may be the case, since the GRP78/BiP signal was abundant in the cell pellets where mutant lysozymes existed (cf. Figs. 2 and 7A). Moreover, our unpublished data using the protein tag technique suggested the association of GRP78/BiP with lysozyme mutants (details will be published elsewhere). At the least, the aforementioned defect in the augmentation of the apoptotic cell ratio in the presence of abundant aberrant lysozymes might be explained by the general role of GRP78/BiP in the restoration of homeostasis. Precise time course experiment was needed since, as noted above, we have obtained indications that apoptotic conditions were aroused after a long time of incubation.

One could argue whether the materials derived from amyloidogenic lysozymes and accumulated in the ER of the present cells are fibrils or not. Our recent experiments showed that the cytoplasm of I56T cells incubated for 72 h after transfection produced strong fluorescence of Thioflavin S, which is said to bind amyloid fibrils, and the signal regions corresponded with those of lysozyme (Suppl. Fig. S2). As seen in this figure, no fluorescence was obtained in the wild-type lysozyme specimen (see "Wild" panels). Also hardly reacted with thioflavin T were the lysates and the culture media for the wild-type cells, as well as the culture media for the mutant cells (data not shown). Nevertheless, it cannot be concluded that the mutant lysozymes form bona fide amyloid fibrils in the ER because of the limitation of the fluorescence method

applied and without the study using fibril specific conformational antibody.

As a whole, our present observations indicate that the overexpression of mutant human lysozyme proteins stimulated ER stress, resulting in UPR activation in cultured cells. Such behavior of human lysozyme variants have been observed previously in *P. pastoris* and *D. melanogaster*[16,17,28]. Novel aspect of the current study using human cell lines is the localization of the aberrant proteins in the ER. Another significant point may be that the gene expression of variant lysozymes correlated not only with the amount of insoluble proteins but also the extent of UPR activation, i.e., the IRE1 system was selectively induced upon the UPR, although the question as to why and how the selection occurred, as well as whether or not such phenomena are also induced by other secretory proteins, is yet a matter of future challenge. Supposedly, the lysozyme variants are incompletely folded and bound, without disassociation, to the mobilized GRP78/BiP, resulting in the formation of insoluble aggregates, which thereby remained accumulated in the ER.

A research goal along this line is to identify the latent pathogenic consequences of the expression of amyloidogenic lysozymes in human cells. Aberrant lysozymes cause systemic amyloidosis when located in organs. The overexpression of amyloidogenic lysozyme (F57I) in *D. melanogaster* has been reported to disrupt the eye development [17]. Although forced overexpression of the amyloidogenic mutant lysozymes leads to their rapid accumulation in the ER, it is estimated, in the case of human body, that the accumulation of the mutant proteins proceeds slowly, resulting in developing amyloidosis mainly in the 40–50's [5,45]. Several diseases including diabetes II [46] and amyotrophic lateral sclerosis (ALS) [47,48] are known to be brought about by the accumulation of misfolding proteins in the ER. A recent report indicated that, in *Saccharomyces cerevisiae*, unstable lysozymes may interact with a calnexin homolog, possibly causing their retention in the ER and subsequent elimination via ER-associated degradation [49]. Amyloidogenic lysozymes might provide fuller information as a common model for diseases. The causative relationship between the pathogenesis of mutant lysozymes and the UPR activation in the ER is an open question, and our experimental system can give insights into the symptom-onset processes of amyloid diseases.

Transparency document

The Transparency document associated with this article can be found, in the online version.

Acknowledgments

This work was supported in part by a Grant-in-Aid for Scientific Research from the Ministry of Education, Culture, Sports, Science, and Technology of Japan (25450476).

Appendix A. Supplementary data

Supplementary data to this article can be found online at http://dx.doi.org/10.1016/j.bbagen.2015.01.018.

References

[1] R. Veerhuis, R.S. Boshuizen, A. Familian, Amyloid associated proteins in Alzheimer's and prion disease, Curr. Drug Targets CNS Neurol. Disord. 4 (2005) 235–248.
[2] D. Aarsland, R. Perry, A. Brown, J.P. Larsen, C. Ballard, Neuropathology of dementia in Parkinson's disease: a prospective, community-based study, Ann. Neurol. 58 (2005) 773–776.
[3] C. Chakraborty, S. Nandi, S. Jana, Prion disease: a deadly disease for protein misfolding, Curr. Pharm. Biotechnol. 6 (2005) 167-177.
[4] J. Montane, A. Klimek-Abercrombie, K.J. Potter, C. Westwell-Roper, B. Verchere, Metabolic stress, IAPP and islet amyloid, Diabetes Obes. Metab. 3 (2012) 68–77.
[5] M.B. Pepys, P.N. Hawkins, D.R. Booth, D.M. Vigushin, G.A. Tennent, A.K. Soutar, et al., Human lysozyme gene mutations cause hereditary systemic amyloidosis, Nature 362 (1993) 553–557.
[6] G.G. Glenner, Amyloid deposits and amyloidosis. The β-fibrilloses, N. Engl. J. Med. 302 (1980) 1333–1343.
[7] L.W. Jin, K.A. Claborn, M. Kurimoto, et al., Imaging linear birefringence and dichroism in cerebral amyloid pathologies, Proc. Natl. Acad. Sci. U. S. A. 100 (2003) 15294–15298.
[8] C.M. Dobson, Protein folding and misfolding, Nature 426 (2003) 884–890.
[9] F. Chiti, C.M. Dobson, Amyloid formation by globular proteins under native conditions, Nat. Chem. Biol. 5 (2009) 15–22.
[10] P. Westermark, M.D. Benson, J.N. Buxbaum, A.S. Cohen, B. Frangione, S. Ikeda, C.L. Masters, G. Merlini, M.J. Saraiva, J.D. Sipe, Amyloid: toward terminology clarification. Report from the Nomenclature Committee of the International Society of Amyloidosis, Amyloid 12 (2005) 1–4.
[11] Y. Aso, K. Shiraki, M. Takagi, Systematic analysis of aggregates from 38 kinds of non disease-related proteins: identifying the intrinsic propensity of polypeptides to form amyloid fibrils, Biosci. Biotechnol. Biochem. 71 (2007) 1313–1321.
[12] C.G. Glabe, Structural classification of toxic amyloid oligomers, J. Biol. Chem. 283 (2008) 29639–29643.
[13] L. Callewaert, C.W. Michiels, Lysozymes in the animal kingdom, J. Biosci. 35 (2010) 127–160.
[14] G. Lesnierowsli, J. Kjowski, Lysozyme, in: R. Huopalahti, R. Lopez-Fandino, M. Anton, R. Schade (Eds.), Bioactive Egg Compounds, Berlin Heidelberg, Springer-Verlag., 2007, pp. 34–42.
[15] G. Merlini, V. Bellotti, Lysozyme: a paradigmatic molecule for the investigation of protein structure, function and misfolding, Clin. Chim. Acta 357 (2005) 168–172.
[16] J.R. Kumita, R.J. Johnson, M.J. Alcocer, M. Dumoulin, F. Holmqvist, M.G. McCammon, C.V. Robinson, D.B. Archer, C.M. Dobson, Impact of the native-state stability of human lysozyme variants on protein secretion by *Pichia pastoris*, FEBS J. 273 (2006) 711–720.
[17] J.R. Kumita, L. Helmfors, J. Williams, L.M. Luheshi, L. Menzer, M. Dumoulin, D.A. Lomas, D.C. Crowther, C.M. Dobson, A.C. Brorsson, Disease-related amyloidogenic variants of human lysozyme trigger the unfolded protein response and disturb eye development in *Drosophila melanogaster*, FASEB J. 26 (2012) 192–202.
[18] K. Takano, J. Funahashi, K. Yutani, The stability and folding process of amyloidogenic mutant human lysozymes, Eur. J. Biochem. 268 (2001) 155–159.
[19] D. Canet, M. Sunde, A.M. Last, A. Miranker, A. Spencer, C.V. Robinson, C.M. Dobson, Mechanistic studies of the folding of human lysozyme and the origin of amyloidogenic behavior in its disease-related variants, Biochemistry 38 (1999) 6419–6427.
[20] M. Dumoulin, J.R. Kumita, C.M. Dobson, Normal and aberrant biological self-assembly: insights from studies of human lysozyme and its amyloidogenic variants, Acc. Chem. Res. 39 (2006) 603–610.
[21] R. Swaminathan, V.K. Ravi, S. Kumar, M.V. Kumar, N. Chandra, Lysozyme: a model protein for amyloid research, Adv. Protein Chem. Struct. Biol. 84 (2011) 63–111.
[22] Y. Sugimoto, Y. Kamada, Y. Tokunaga, H. Shinohara, M. Matsumoto, T. Kusakabe, T. Ohkuri, T, Ueda, Aggregates with lysozyme and ovalbumin show features of amyloid-like fibrils, Biochem. Cell Biol. 89 (2011) 533–544.
[23] Y. Tokunaga, Y. Sakakibara, Y. Kamada, K. Watanabe, Y. Sugimoto, Analysis of core region from egg white lysozyme forming amyloid fibrils, Int. J. Biol. Sci. 9 (2013) 219–227.
[24] S. Goda, K. Takano, Y. Yamagata, S. Maki, K. Namba, K. Yutani, Elongation in a beta-structure promotes amyloid-like fibril formation of human lysozyme, J. Biochem. 132 (2002) 655–661.
[25] M. Sunde, C.C.F. Blake, Instability, unfolding and aggregation of human lysozyme variants underlying amyloid fibrillogenesis, Nature 385 (1997) 787–793.
[26] A.L. Gharibyan, V. Zamotin, K. Yanamandra, O.S. Moskaleva, B.A. Margulis, I.A. Kostanyan, L.A. Morozova-Roche, Lysozyme amyloid oligomers and fibrils induce cellular death via different apoptotic/necrotic pathways, J. Mol. Biol. 365 (2007) 1337–1349.
[27] M. Otsu, R. Omura, M.T. Yoshimori, M. Kikuchi, Protein disulfide isomerase associates with misfolded human lysozyme in vivo, J. Biol. Chem. 269 (1994) 6874–6877.
[28] G. Whyteside, M.J.C. Alcocer, J.R. Kumita, C.M. Dobson, M. Lazarou, R.J. Pleass, D.B. Archer, Native-state stability determines the extent of degradation relative to secretion of protein variants from *Pichia pastoris*, PLoS ONE 6 (2011) e22692 (doi: 10.1371).
[29] G. Esposito, J. Garcia, P. Mangione, S. Giorgetti, A. Corazza, P. Viglino, F. Chiti, A. Andreola, P. Dumy, D. Booth, P.N. Hawkins, S. Bellotti, Structural and folding dynamic properties of the T70N variant of human lysozyme, J. Biol. Chem. 278 (2003) 25910–25918.
[30] Y. Kawaguchi, J. Kovacs, A. McLaurin, J.M. Vance, A. Ito, T.P. Yao, The deacetylase HDAC6 regulates aggresome formation and cell viability in response to misfolded protein stress, Cell 115 (2003) 727–738.
[31] H. Ouyang, Y.O. Ali, M. Ravichandran, A. Dong, W. Qiu, F. MacKenzie, S. Dhe- aganon, C.H. Arrowsmith, R.G. Zhai, Protein aggregates are recruited to aggresome by histone deacetylase 6 via unanchored ubiquitin C termini, J. Biol. Chem. 287 (2012) 2317–2327.
[32] N.G. Bauer, C. Richter-Landsberg, The dynamic instability of microtubules is required for aggresome formation in oligodendroglial cells after proteolytic stress, J. Mol. Neurosci. 29 (2006) 153–168.
[33] S.J. Marciniak, D. Ron, Endoplasmic reticulum stress signaling in disease, Physiol. Rev. 86 (2006) 1133–1149.
[34] K. Mori, Signalling pathways in the unfolded protein response: development from yeast to mammals, J. Biochem. 146 (2009) 743–750.
[35] A. Chakrabarti, A.W. Chen, J.D. Varner, A review of the mammalian unfolded protein response, Biotechnol. Bioeng. 108 (2011) 2777–2793.
[36] C.W. Lai, J.H. Otero, L.M. Hendershot, E. Snapp, ERdj4 protein is a soluble endoplasmic reticulum (ER) DnaJ family protein that interacts with ER-associated degradation machinery, J. Biol. Chem. 287 (2012) 7969–7978.

[37] M. Ni, H. Zhou, S. Wey, P. Baumeister, A.S. Lee, Regulation of PERK signaling and leukemic cell survival by a novel cytosolic isoform of the UPR regulator GRP78/BiP, PLoS ONE 4 (2009) e6868.
[38] J. Maiuolo, S. Bulotta, C. Verderio, R. Benfante, N. Borgese, Selective activation of the transcription factor ATF6 mediates endoplasmic reticulum proliferation triggered by a membrane protein, Proc. Natl. Acad. Sci. U. S. A. 108 (2011) 7832–7837.
[39] J. Hollien, Evolution of the unfolded protein response, Biochim. Biophys. Acta 1833 (2013) 2458–2463.
[40] A. Uemura, M. Oku, K. Mori, H. Yoshida, Unconventional splicing of XBP1 mRNA occurs in the cytoplasm during the mammalian unfolded protein response, J. Cell Sci. 122 (2009) 2877–2886.
[41] C. Gallerne, A. Prola, C. Lemaire, Hsp90 inhibition by PU-H71 induces apoptosis through endoplasmic reticulum stress and mitochondrial pathway in cancer cells and overcomes the resistance conferred by Bcl-2, Biochim. Biophys. Acta 1833 (2013) 1356–1366.
[42] R.J. Viana, C.J. Steer, C.M. Rodrigues, Amyloid-β peptide-induced secretion of endoplasmic reticulum chaperone glycoprotein GRP94, J. Alzheimers Dis. 27 (2011) 61–73.
[43] H. Nishitoh, CHOP is a multifunctional transcription factor in the ER stress response, J. Biochem. 151 (2012) 217–219.
[44] M. Misiewicz, M.A. Déry, B. Foveau, J. Jodoin, D. Ruths, A.C. LeBlanc, Identification of a novel endoplasmic reticulum stress response element regulated by XBP1, J. Biol. Chem. 288 (2013) 20378–20391.
[45] P.T. Sattianayagam, S.D.J. Gibbs, D. Rowczenio, J.H. Pinney, A.D. Wechalekar, J.A. Gilbertson, P.N. Hawkins, H.J. Lachmann, J.D. Gillmore, Hereditary lysozyme amyloidosis — phenotypic heterogeneity and the role of solid organ transplantation, J. Int. Med. 272 (2012) 36–44.
[46] S. Matus, V. Valenzuela, D.B. Medinas, C. Hetz, ER dysfunction and protein folding stress in ALS, Int. J. Cell Biol. 2013 (2013) (ID 674751).
[47] R. Chandra, R.A. Liddle, Modulation of pancreatic exocrine and endocrine secretion, Curr. Opin. Gastroenterol. 9 (2013) 517–522.
[48] T. Prell, J. Lautenschläger, J. Grosskreutz, Calcium-dependent protein folding in amyotrophic lateral sclerosis, Cell Calcium 54 (2013) 132–143.
[49] H. Azakami, M. Uehara, R. Matsuo, Y. Tsurunaga, Y. Yamashita, M. Usui, A. Kato, Unstable mutant lysozymes are degraded through the interaction with calnexin homolog Cne1p in *Saccharomyces cerevisiae*, Biosci. Biotechnol. Biochem. 78 (2014) 1263–1269.